Published in final edited form as:
Small. 2013 May 27; 9(0): . doi:10.1002/smll.201201510.

Multistage Vectored siRNA Targeting Ataxia-Telangiectasia Mutated for Breast Cancer Therapy

Rong Xu,
Department of Nanomedicine, The Methodist Hospital Research Institute, 6670 Bertner Avenue, Houston, Texas 77030, USA

Yi Huang,
Department of Nanomedicine, The Methodist Hospital Research Institute, 6670 Bertner Avenue, Houston, Texas 77030, USA

Junhua Mai,
Department of Nanomedicine, The Methodist Hospital Research Institute, 6670 Bertner Avenue, Houston, Texas 77030, USA

Guodong Zhang,
Department of Nanomedicine, The Methodist Hospital Research Institute, 6670 Bertner Avenue, Houston, Texas 77030, USA

Xiaojing Guo,
Department of Nanomedicine, The Methodist Hospital Research Institute, 6670 Bertner Avenue, Houston, Texas 77030, USA & Department of Breast Pathology, Cancer Hospital of Tianjin Medical University, Tianjin 300060, China

Xiaojun Xia,
Department of Nanomedicine, The Methodist Hospital Research Institute, 6670 Bertner Avenue, Houston, Texas 77030, USA

Eugene J Koay,
Department of Nanomedicine, The Methodist Hospital Research Institute, 6670 Bertner Avenue, Houston, Texas 77030, USA & Division of Radiation Oncology, The University of Texas M. D. Anderson Cancer Center, 1515 Holcombe Blvd., Houston, TX, 77030

Qingpo Li,
Department of Nanomedicine, The Methodist Hospital Research Institute, 6670 Bertner Avenue, Houston, Texas 77030, USA

Xuewu Liu,
Department of Nanomedicine, The Methodist Hospital Research Institute, 6670 Bertner Avenue, Houston, Texas 77030, USA

Mauro Ferrari[*], and
Department of Nanomedicine, The Methodist Hospital Research Institute, 6670 Bertner Avenue, Houston, Texas 77030, USA & Department of Medicine, Weill Cornell Medical College, New York, NY 10065, USA

Haifa Shen[*]

[*]mferrari@tmhs.orghshen@tmhs.org.

Current address: Drug R&D center, Hangzhou Minsheng Pharmaceutical Co., Ltd., Hangzhou, China

The other authors disclosed no potential conflicts of interest.

Department of Nanomedicine, The Methodist Hospital Research Institute, 6670 Bertner Avenue, Houston, Texas 77030, USA & Department of Cell and Developmental Biology, Weill Cornell Medical College, New York, NY 10065, USA

Abstract

The ataxia-telangiectasia mutated (ATM) protein plays a central role in DNA damage response and cell cycle checkpoints, and may be a promising target for cancer therapy if normal tissue toxicity could be avoided. Our strategy to target ATM for breast cancer therapy involves the use of liposomal-encapsulated, gene-specific ATM small interfering RNA (siRNA) delivered with a well-characterized porous silicon-based multistage vector (MSV) delivery system (MSV/ATM). Here we have shown that biweekly treatment of MSV/ATM suppressed ATM expression in tumor tissues, and consequently inhibited growth of MDA-MB-231 orthotopic tumor in nude mice. At the therapeutic dosage, neither free liposomal ATM siRNA nor MSV/ATM triggered acute immune response in BALB/c mice, including changes in serum cytokines, chemokines or colony-stimulating factors. Weekly treatments of mice with free liposomal ATM siRNA or MSV/ATM for 4 weeks did not cause significant changes in body weight, hematology, blood biochemistry, or major organ histology. These results indicate that MSV/ATM is biocompatible and efficacious in inhibiting tumor growth, and that further preclinical evaluation is warranted for the development of MSV/ATM as a potential therapeutic agent.

Keywords

ATM; breast cancer; delivery; multistage vector; siRNA; toxicity

1. Introduction

Triple negative breast cancer (TNBC) cells lack the expression of estrogen receptor, progesterone receptor, and Her2/neu. TNBC patients have the lowest five-year survival rate among all breast cancer types due to local recurrence and metastasis [1]. Therapeutic options are limited for TNBC because these cancers do not respond to most systemic agents including therapies targeting the estrogen receptor or Her2/neu, or chemotherapy, making TNBC a very difficult disease to fight.

Recent advances in the development of targeted therapy drugs have proven the effectiveness of targeting the DNA damage response pathways to fight TNBC [2]. Mammalian cells are continuously exposed to DNA damage. It is essential that cells have DNA repair mechanism in place to preserve genomic integrity. These include homologous recombination where ataxia-telangiectasia mutated (ATM) and subsequently BRCA1 play essential roles, and base excision repair that requires poly (ADP-ribose) polymerase (PARP) activity. Small molecule PARP inhibitors have recently been successfully developed to treat patients with hereditary breast cancer and hereditary ovarian cancer carrying BRCA1 mutations [3]. Therapeutic agents that target ATM are also expected to have a major impact on breast cancer therapy. ATM is a serine/threonine protein kinase. In response to DNA damage, the ATM kinase phosphorylates downstream targets such as p53, CHK2, and BRCA1, and regulates DNA repair and cell cycle checkpoints. Cells with a defective ATM gene are hypersensitive to DNA-damaging agents. Multiple studies have already shown the effectiveness of targeting the ATM gene with small inhibitory RNA (siRNA) oligos in vitro to inhibit breast cancer growth [4].

While siRNA is effective to treat tumor cells *in vitro*, it is difficult to deliver siRNA therapeutic to solid tumors. Tissue-specific delivery remains a major challenge to the wide-

spread application of siRNA therapeutics [5]. The central problem for delivery of siRNA is the existence of multiple biological barriers inside the body that prevent siRNA from reaching the target tumor tissue [6]. These barriers include organs of the reticulo-endothelial system (RES), enzymatic degradation of siRNA by plasma and tissue RNases, and high tumor interstitial pressure inside the tumor tissue. We have developed a porous silicon particle-based multistage vector (MSV) delivery system to overcome the biological barriers of cancer in order to deliver enough therapeutics and imaging agents to tumor tissues [7]. This system comprises of nanoporous silicon microparticles (first-stage particles) loaded with drug-incorporated nanoparticles (second-stage particles). Following injection into the systemic circulation, the particles travel in the circulation and accumulate in tumor vasculature where secondary nanoparticles are released through diffusion from the slowly degrading porous silicon particles to achieve sustained release of the therapeutics. The nanoparticles then traverse the tumor interstitium and are internalized by tumor cells for drug action. Our previous findings indicate that approximately 6-10% of total particles settle in the tumor vasculature [8], providing a dramatic improvement from the less than 0.1% accumulation observed in tumor tissue by conventional means of delivery of biological agents [9]. Using this system, we have successfully delivered siRNA oligos, and demonstrated superb therapeutic efficacy on tumor growth inhibition with mouse models of human ovarian cancer [10].

It has been well documented that systemic delivery of siRNA oligos might cause undesirable side effects, most notably innate immune response by triggering toll-like receptor 3, 7, and 8 pathways [11]. Interaction between nanoparticles and cells also play key roles in cytotoxicity [12]. It is thus very important to assess the toxicity profile of a multistage vectored ATM siRNA (MSV/ATM) before any other resources are committed for a full-scale product development effort. In the current study, we incorporated ATM siRNA into 1,2-dioleoyl-*sn*-glycero-3-phosphocholine (DOPC) neutral nanoliposomes, and subsequently loaded them into MSV. Athymic nude mice bearing MDA-MB-231 primary tumor were treated with MSV/ATM to test therapeutic efficacy. BALB/c mice were treated once with escalating dosages of either free siRNA nanoliposomes or MSV/siRNA, and serum cytokine and chemokine levels were measured to assess potential innate immune response. Mice were also treated weekly with repetitive dosages of either free siRNA nanoliposomes or MSV/siRNA for 4 weeks, and potential damages to major organs and the hematopoietic system were evaluated. Based on these studies, we have concluded that the nanotechnology-based MSV/ATM is a safe product for potential cancer treatment applications.

2. Results

2.1. Characterization of nanoparticles and sustained release of siRNA in cancer cells

The discoidal porous silicon microparticles were fabricated by a combination of photolithography and electrochemical etch, and conjugated with 3-aminopropyltriethoxysilane (APTES) on surface to increase stability [13]. They were 1 □m in diameter and 700 nm in height. The siRNA oligos were packaged into DOPC nanoliposomes, and loaded into the nanopores inside porous silicon. The empty silicon particles carried a positive surface charge, and became negatively charged once the slightly negatively charged nanoliposomes were loaded (Table 1).

To investigate cellular uptake of MSV/siRNA and subsequent release of siRNA oligos from MSV, we packaged Alexa 555-conjugated siRNA into nanoliposomes (Alexa 555-siRNA) and loaded them into MSV (MSV/Alexa 555-siRNA). Human breast cancer cells MDA-MB-231 and SK-BR-3 were incubated with MSV/Alexa555-siRNA, and release of siRNA was monitored over the next 11 days (Figure 1). Confocal microscopic analysis revealed that multiple MSV/Alexa555-siRNA particles could be uptaken by the cells. Strong fluorescent

intensity from Alexa555-siRNA could be visualized within or around the silicon particles on day 1 and day 7. The red fluorescent siRNA could still be detected in these cells on day 11. This result indicates that the MSV particles are stable inside the cells, and that sustained release of siRNA oligo from the MSV can be achieved.

2.2. MSV/ATM inhibits growth of human breast cancer xenografts

Mice bearing orthotopic MDA-MB-231 breast cancer were divided into 3 groups. They were treated with phosphate buffer saline or MSV loaded with liposomes packaged with scramble control siRNA (MSV/Scr) in the control groups, or MSV/ATM in the treatment group. Treatment initiated when the average tumor size reached 150 – 200 mm^3, and all mice were sacrificed 4 weeks after the first treatment due to rapid tumor growth in the control groups. At the end of the study, average tumor weight was 0.996 g in the PBS group, 0.820 g in the MSV/Scr group, and 0.334 g in the MSV/ATM group (Fig. 2). Immunohistochemical staining revealed that ATM expression was still dramatically inhibited in the tumor mice treated with MSV/ATM 17 days after the last treatment (Fig. 2c).

2.3. MSV/ATM does not trigger innate immune response

One of the major concerns on siRNA therapeutics is activation of innate immune response since naked siRNA oligos can induce production of high levels of pro-inflammatory cytokines such as tumor necrosis factor alpha (TNF- □), interleukin-6 (IL-6) and interferons [11]. We have previously shown that the porous silicon microparticles alone did not cause any significant toxicity [14]. In the current study, we set up experiments to determine whether the siRNA-loaded MSV particles would trigger immune responses *in vitro* and *in vivo*. We co-incubated MSV/ATM with Raw-264.7 mouse macrophage cells for 2 or 24 hours, and measured TNF- □production by ELISA. Polyinosinic: polycytidylic acid (poly I:C) and lipopolysaccharide (LPS) were used as the positive control, as their potential to induce innate immune response has been well documented [15]. While treatment with the poly I:C or LPS caused a significant induction of TNF- □, level of this cytokine was not elevated in cells treated with free ATM siRNA liposomes or MSV/ATM (Figure 3a). We also assessed expression levels of the interferon responsive genes OAS1 and STAT1 by real-time quantitative reverse transcriptase-PCR (RT-PCR). Neither poly I:C nor LPS caused significant expression of these genes 2 hours after treatment (data not shown). At the 24-hour time point, however, LPS treatment dramatically stimulated OAS1 and STAT1 expression. On the other hand, treatment with free siRNA liposomes or MSV/ATM did not have any effect on expression of TNF- □, OAS1, or STAT1 (Fig. 3b).

To evaluate potential innate immune activation *in vivo*, we treated BALB/c mice with free liposomal siRNA or MSV-loaded siRNA, and performed a multiplexed bead-based assay to measure levels of 32 cytokines/chemokines/colony stimulating factors. Many of these factors are involved in the initial steps of the innate immune response and promote the development and trafficking of various subsets of immune and non-immune cells [16]. So this analysis should provide a comprehensive view of the host reaction to siRNA therapeutics. As expected, treatment with the positive control poly I:C or LPS resulted in increase of most of the cytokines /chemokines/colony-stimulating factors (Fig. 3c and Supplementary Fig. 1). Treatment with a therapeutic dose of MSV/ATM (15 □g siRNA) or free nanoliposomal siRNA did not trigger induction of immune response (Fig. 3c and Supplementary Fig. 1). Treatment with 75 □g scramble siRNA or ATM siRNA in MSV caused significant increase in two (IL-10 and MCP-1) of the 32 factors (Fig. 3c). However, the amount of MSV particles and siRNA oligos in these groups was 5 folds as high as the therapeutic dosage (Fig. 2).

2.4. MSV/ATM does not cause sub-acute toxicity

To evaluate sub-acute toxicity, we treated mice once a week with 15 μg or 75 μg siRNA packaged in free nanoliposomes or loaded into MSV for 4 weeks by systemic delivery. No apparent toxicity or animal death occurred during the entire treatment period. There was no body weight change or behavior change either. Mice were sacrificed at the end of the 4-week treatment, and major organs including the heart, liver, lung, spleen, kidney, and brain were collected. Table 2 summarizes the relative weights of liver, spleen, and kidneys compared to total body weight (wet weight of the tissue/body weight, in mg/g). No significant difference was found.

We carried out hematological analysis to assess any abnormality in mice treated with ATM siRNA. The hematological values of ATM siRNA-treated mice were not significantly different from those in the PBS-treated group (Fig. 4). In contrast, treatment with poly I:C resulted in a dramatic decrease in the number of total white blood cells, lymphocytes, granulocytes and monocytes, although only the granulocyte count was dropped to below the normal range (Fig. 4a). This result was in consistency with previous reports [17]. None of these treatments affect the levels of red blood cells, hemoglobin concentration, or platelet counts (Fig. 4b).

We evaluated biochemical parameters to assess potential damage to the functions of major organs (Fig. 5 and Supplementary Fig. 2). Biomarkers for liver function included aspartate aminotransferase (AST), alanine aminotransferase (ALT), albumin (ALB), and alkaline phosphatase (ALKP) (Fig. 5a). Parameters for renal function were blood urea nitrogen (BUN), and serum concentrations of creatinine, and Na^+, K^+, and Cl^- (Fig. 5b). Other biomarkers included activities of lactate dehydrogenase (LDH), creatinine kinase MB (CK-MB), Amylase (Amyl) and cholinesterase (CHE). No change in the above biomarkers was observed in the rest treatment groups.

Histological examination of the heart, liver, spleen, lung and kidney from all treatment groups was preformed. There were no apparent morphological changes based on H&E staining of tissue blocks (Fig. 6 and Supplementary Fig. 3).

3. Discussion

Targeting DNA damage response pathways has proven to be an effective approach to sensitize cancer treatment [2c]. The ATM serine kinase activates the downstream checkpoint kinases and DNA double-strand repair pathways, and plays an essential role in coordinating DNA repair, cell cycle progression, and apoptosis in response to DNA damage. It is not surprising that small molecule inhibitors targeting the ATM kinase have been developed based on their inhibition of serine phosphorylation, and their potential as cancer therapy agents is being evaluated in preclinical studies [18]. It has been demonstrated, however, that serine phosphorylation is dispensible for ATM activation [19], implying that the observed effect on DNA damage response from some of the small molecule inhibitors might be an off-target effect through inhibition of other important kinases. It has been reported that STAT3 phosphorylation can be blocked by the ATM inhibitor KU55933 [20]. KU55933 is also a potent inhibitor of AKT phosphorylation [21]. It has also been reported that a defective ATM serves as a dominant-negative protein in a mouse knock-in model [22]. As a result, inhibition of the ATM kinase activity with small molecule inhibitors might cause adverse consequences to the body. Treating tumor cells with ATM siRNA knocks down the amount of ATM protein, and consequently the overall ATM kinase activity, and thus might represent an alternative approach to develop a safe and effective targeted therapy.

In the current study, we have shown that MSV/ATM is effective in knocking down of ATM expression *in vivo*, which results in significant growth inhibition of MDA-MB-231 xenograft tumor. The result is surprising in that no combination treatment with radiation or chemotherapy drug is involved in the study. A possible reason for the superb efficacy from MSV/ATM is that MDA-MB-231 is a cell line with a mutant p53 protein. A recent study demonstrated synergy between inhibition of ATM and p53 mutation in human cancer cells [4b]. It remains to be seen if MSV/ATM is effective in other cancer cell lines with a deficient p53. If proven to be the case, this agent will have broad applications in cancer therapy, since p53 is mutated in over 20% of breast cancer cases [23], and in over 60% of colon cancer, lung cancer, and stomach cancer cases [24].

One major concern on siRNA therapeutics is their potential toxicity including the possibility of triggering innate immune response by the siRNA oligos [5]. So we evaluated acute and sub-acute toxicity from nanoliposomal ATM siRNA and MSV/ATM siRNA. No sub-acute toxicity was observed from mice treated with the therapeutic dose (15 μg siRNA in free liposomes or in MSV) or the supra-therapeutic dose (75 μg siRNA). Results from the acute toxicity study showed no significant changes among the 32 cytokines, chemokines, and colony stimulating factors after the mice were treated with a therapeutic dosage of siRNA, indicating that no innate immune response was triggered by either MSV/siRNA or free nanoliposomal siRNA. Levels of IL-10 and MCP-1 were elevated upon treatment with 75 μg scramble siRNA or ATM siRNA in MSV. Interestingly, IL-10 is an anti-inflammatory cytokine. It has been reported that certain types of nanoparticles can activate signals in the spleen to produce IL-10 if mice are administrated with a large quantity of particles [25]. On the other hand, MCP-1 can induce tumor infiltration of monocytes/macrophages [26]. Our previous work has shown that macrophages are very efficient in uptaking porous silicon particles [27]. A surge in MCP-1 level might facilitate tumor enrichment of MSV particles via these cells, and thus tumor-specific delivery of siRNA therapeutics.

4. Conclusion

Any unwanted immunogenic responses from a drug can result in clinical events ranging from lack of therapeutic efficacy to severe adverse events. To our knowledge, this is the first systematic study to evaluate the efficacy and acute and sub-acute toxicities with a candidate siRNA therapeutic agent in nanoformulation targeting the DNA damage response pathways. We have demonstrated that ATM expression can be effectively knocked down by gene-specific siRNA, which results in tumor growth inhibition *in vivo*. There is no acute or sub-acute toxicity from ATM siRNA oligo delivered in free nanoliposomes or loaded in the porous silicon-based multistage vector delivery system, indicating safe application of ATM siRNA therapeutics for cancer treatment.

5. Experimental Section

Materials

All chemicals for silicon microparticle fabrication, poly I:C sodium salt and lipopolysaccharides were purchased from Sigma-Aldrich. Alexa Fluor 555-labeled siRNA was obtained from QIAGEN. The scramble siRNA (sense: 5′-CUCAUAGGAAGACCCCAUU, antisense: 5′-AAUGGGGUCUUCCUAUGAG) and the human ATM gene-specific siRNA (sense: 5′-GGCCCUUAAGUUAUUUGAAGAUA, anti-sense: 5′-UAUCUUCAAAUAACUUAAGGGCC) were purchased from Sigma-Aldrich. Primers for quantitative RT-PCR: STAT1 (forward primer: 5′-TCACAGTGGTTCGAGCTTCAG, reverse primer: 5′-GCAAACGAGACATCATAGGCA), OAS1 (forward primer: 5′-CCAAGGTGGTGAAGGGTGG, reverse primer: 5′-ACCACCAGGTCAGCGTCTGA), 2′

actin (forward primer: 5 AGAGGGAAATCGTGCGTGAC, reverse primer: 5 CAATAGTGATGACCTGGCCGT) were purchased from Sigma-Aldrich. Mouse anti-ATM mAb was from Abcam. Mouse TNF- ELISA kit was purchased from Ebioscience. MILLIPLEX Map Kit with 32plex Mouse Cytokine/Chemokine was purchased from Millipore. RNeasy Mini Kit was obtained from Qiagen. TaqMan® Reverse Transcription Reagents Kit was purchased from Roche Applied Science.

Preparation of nanoliposomal siRNA and assembly of MSV/siRNA

Preparation of siRNA nanoliposomes has been described previously [10a]. Fabrication of porous silicon microparticles was carried out based on a combination of photolithography and electrochemical etch [13]. The silicon particles were conjugated with 3-aminopropyltriethoxysilane (APTES), and the slightly negatively charged nanoliposomes were loaded into the positively charged porous silicon particles by mixing followed by a brief sonication. Size of siRNA-loaded liposomes was measured using dynamic light scattering on a ZetaPLUS particle electrophoresis system (Brookhaven Instruments Corp., Holtsville, NY). Zeta ( ) potential for the siRNA-loaded liposome and MSV/siRNA was determined with the ZetaPLUS system.

Fluorescence microscopy

To investigate the intracellular uptake of the MSV delivery of siRNA, MDA-MB-231 and SK-BR-3 human breast cancer cells were incubated with MSV/Alexa Fluor 555-labeled siRNA liposomes. Cells were plated in 2-well chambers at a density of 5×10^3 to 5×10^4 cells per well. They were allowed to grow overnight and before MSV/siRNA was added. Fluorescent images were captured on an Olympus Fluo View TM 1000 laser scanning confocal microscope (Center Valley, PA).

In vivo tumor growth study

The animal studies were performed in accordance with the guidelines of the Animal Welfare Act and the Guide for the Care and Use of Laboratory Animals following protocols approved by the Institutional Animal Care and Use Committee (IACUC). Six week old female athymic nude mice were purchased from Charles River Laboratories (Boston, MA, USA). MDA-MB-231 breast cancer cells (3×10^6) were harvested from exponential cultures and inoculated in the fourth mammary fat pad of nude mice. When the tumor size reaches 150 mm^3, the mice were randomly divided into three groups (n=5), and dosed *i.v.* with 100 PBS, MSV/Scr (15 g siRNA), or MSV/ATM (15 g siRNA). Each animal received 2 treatments (day 1 and day 15). Mice were euthanized on day 32, and tumor tissues were removed. For immunohistochemical staining, tumor sections were incubated with anti-ATM monoclonal antibody (1:100) overnight at 4°C, and then hybridized with a biotinylated goat anti-mouse IgG second antibody for 30 min at 37°C.

In vitro tumor necrosis factor-α secretion assay

Raw 264.7 murine macrophage cells were seeded in a 96-well plate with a density of 3×10^4 cells/well. Cells were incubated with various agents including the poly I:C and LPS positive controls, free liposomal siRNA oligos and MSV/siRNA for 2 or 24 hours at 37°C. At the end of incubation, supernatants were collected, and TNF- level was measured using an ELISA kit.

Quantitative RT-PCR

Total RNA from cells was isolated using the RNeasy Mini Kit. cDNA synthesis was performed following the manufacturer's instruction of the TaqMan® Reverse Transcription Reagents Kit. Quantitative RT-PCR was carried out on a LightCycler (Roche Applied

Science, USA). For amplification of specific transcripts, primers for OAS1, STAT1 and β-actin were applied according to the manufacturer's instructions. Expression ratios of the target genes were normalized with the expression of β-actin.

Toxicity evaluation in vivo

Healthy 6 to 8 week old female BALB/c mice were purchased from Charles River Laboratories and maintained in a pathogen-free facility under a 12 hour light – 12 hour dark cycle. In the acute toxicity study, mice were randomly divided into treatment groups (n = 3). Mice were dosed via tail vein injection with either free liposomal siRNA or MSV/siRNA (15 μg siRNA in the low dosage treatment and 75 μg siRNA in the high dosage treatment groups). Mice in the positive control group received intraperitoneal injection of poly I:C (100 μg), or LPS (5 mg/kg) reconstituted in sterile and endotoxin-free phosphate-buffered saline. In the first experiment with poly I:C the positive control, blood samples were collected 3 and 6 hours after dosing. In the second experiment with LPS as the positive control, samples were collected 2 and 24 hours after treatment. All blood samples were collected by retro-orbital bleeding for analysis of cytokines/chemokines/colony-stimulating factors production. In the sub-acute toxicity study, mice received *i.v.* injection of the reagents weekly for 4 weeks. General conditions were observed during the treatments such as general activity, breathing, reflection, spasm, skin and hair, eyes, discharge, and secretion. Blood samples were collected 24 hours after the last dosing by eye bleeding, and analyzed for whole blood hematological test and serum chemical analysis. The major organs (heart, liver, spleen, lung and kidney) were harvested, fixed in 10% formalin, and processed by hematoxylin/eosin (H&E) staining for histological evaluation.

Cytokines, chemokines and colony stimulating factors analysis

Serum levels of cytokines, chemokines and colony-stimulating factors were measured using a multiplexed bead-based immunoassay from Milliplex, which simultaneously detected 32 pro- and anti-inflammatory cytokines [IL-1α, IL-1β, IL-2, IL-3, IL-4, IL-5, IL-6, IL-7, IL-9, IL-10, IL-12 (p40), IL-12 (p70), IL-13, IL-15, IL-17, interferon-γ(IFNγ), TNFa and leukemia inhibitory factor (LIF)], chemokines [eotaxin, MCP-1, macrophage inflammatory protein-1α(MIP-1a), MIP-1β, regulated on activation normal T cells expressed and secreted (RANTES), interferon inducible protein 10 (IP-10), keratinocyte derived chemokine (KC), lipopolysaccharide (LPS) induced CXC chemokine (LIX), monokine induced by gammainterferon (MIG) and MIP-2], and colony stimulating factors [granulocyte-macrophage (GM)-CSF, granulocyte (G)-CSF, macrophage (M)-CSF and vascular endothelial growth factor (VEGF)] on Luminex 200 analyzer.

Whole blood analysis

Blood samples were collected from mice 24 hours after the last injection in the sub-acute toxicity groups. The samples were analyzed for the number and percentage of total white blood cells (WBC), lymphocytes (LYM), monocytes (MON), granulocytes (GRAN). Red blood cell count (RBC) and hemoglobin content (HGB), hematocrit value (HCT), mean corpuscular volume (MCV), mean corpuscular hemoglobin (MCH), mean cell hemoglobin concentration (MCHC), red cell distribution width (RDW), platelets count (PLT), mean platelet volume (MPV) were also measured.

Blood biochemistry

Serum samples were analyzed to measure parameters for hepatic function (ALB, ALKP, ALT, and AST), renal function (BUN, creatinine, Na^+, K^+, and Cl^-), and others including CKMB, lactate LDH, Amyl and CHE.

Histopathological examinations

Histopathological analysis was carried out with major organs such as lung, liver, kidney, heart, spleen, brain. Tissue samples were embedded in paraffin blocks and processed. Tissue sections were stained with hematoxylin/eosin. Microscopic analysis was performed to evaluate morphologic changes. At least 5 random sections from each slide were examined.

Statistics

Student's *t* test was performed for statistical comparisons (two-tailed distribution, two-sample equal variance). A value of $P < 0.05$ was considered statistically significant, and a value of $P < 0.01$ was considered statistically very significant.

Supplementary Material

Refer to Web version on PubMed Central for supplementary material.

Acknowledgments

The authors acknowledge financial support from the following sources: Department of Defense grant W81XWH-09-1-0212, the CPRIT grant RP121071 from the state of Texas, National Institute of Health grants U54CA143837 and U54CA151668, and the Ernest Cockrell Jr. Distinguished Endowed Chair. M. Ferrari is the founding scientist and a member of the Board of Directors of Leonardo Biosystems, a member of Board of Directors of Arrow Head Research Corporation, and hereby discloses potential financial interests in the companies.

REFERENCES

1. a Liedtke C, Mazouni C, Hess KR, Andre F, Tordai A, Mejia JA, Symmans WF, Gonzalez-Angulo AM, Hennessy B, Green M, Cristofanilli M, Hortobagyi GN, Pusztai L. J Clin Oncol. 2008; 26:1275–1281. [PubMed: 18250347] b Anderson WF, Chen BE, Jatoi I, Rosenberg PS. Breast Cancer Res Treat. 2006; 100:121–126. [PubMed: 16685588] c Hayes DF, Thor AD, Dressler LG, Weaver D, Edgerton S, Cowan D, Broadwater G, Goldstein LJ, Martino S, Ingle JN, Henderson IC, Norton L, Winer EP, Hudis CA, Ellis MJ, Berry DA. N Engl J Med. 2007; 357:1496–1506. [PubMed: 17928597] d Lin NU, Claus E, Sohl J, Razzak AR, Arnaout A, Winer EP. Cancer. 2008; 113:2638–2645. [PubMed: 18833576]
2. a Tutt A. J. Glendenning. Breast. 2011; 20(Suppl 3):S12–19.b Telli ML, Ford JM. Clin Breast Cancer. 2010; 10(Suppl 1):E16–22. [PubMed: 20587403] c Lord CJ, Ashworth A. Nature. 2012; 481:287–294. [PubMed: 22258607]
3. a Fong PC, Boss DS, Yap TA, Tutt A, Wu P, Mergui-Roelvink M, Mortimer P, Swaisland H, Lau A, O'Connor MJ, Ashworth A, Carmichael J, Kaye SB, Schellens JH, de Bono JS. N Engl J Med. 2009; 361:123–134. [PubMed: 19553641] b Audeh MW, Carmichael J, Penson RT, Friedlander M, Powell B, Bell-McGuinn KM, Scott C, Weitzel JN, Oaknin A, Loman N, Lu K, Schmutzler RK, Matulonis U, Wickens M, Tutt A. Lancet. 2010; 376:245–251. [PubMed: 20609468] c O'Shaughnessy J, Osborne C, Pippen JE, Yoffe M, Patt D, Rocha C, Koo IC, Sherman BM, Bradley C. N Engl J Med. 2011; 364:205–214. [PubMed: 21208101] d Donawho CK, Luo Y, Penning TD, Bauch JL, Bouska JJ, Bontcheva-Diaz VD, Cox BF, DeWeese TL, Dillehay LE, Ferguson DC, Ghoreishi-Haack NS, Grimm DR, Guan R, Han EK, Holley-Shanks RR, Hristov B, Idler KB, Jarvis K, Johnson EF, Kleinberg LR, Klinghofer V, Lasko LM, Liu X, Marsh KC, McGonigal TP, Meulbroek JA, Olson AM, Palma JP, Rodriguez LE, Shi Y, Stavropoulos JA, Tsurutani AC, Zhu GD, Rosenberg SH, Giranda VL, Frost DJ. Clin Cancer Res. 2007; 13:2728–2737. [PubMed: 17473206] e Kummar S, Kinders R, Gutierrez ME, Rubinstein L, Parchment RE, Phillips LR, Ji J, Monks A, Low JA, Chen A, Murgo AJ, Collins J, Steinberg SM, Eliopoulos H, Giranda VL, Gordon G, Helman L, Wiltrout R, Tomaszewski JE, Doroshow JH. J Clin Oncol. 2009; 27:2705–2711. [PubMed: 19364967]
4. a Fujimaki S, Matsuda Y, Wakai T, Sanpei A, Kubota M, Takamura M, Yamagiwa S, Yano M, Ohkoshi S, Aoyagi Y. Cancer Lett. 2012; 319:98–108. [PubMed: 22265862] b Jiang H, Reinhardt HC, Bartkova J, Tommiska J, Blomqvist C, Nevanlinna H, Bartek J, Yaffe MB, Hemann MT.

Genes Dev. 2009; 23:1895–1909. [PubMed: 19608766] c Sun M, Guo X, Qian X, Wang H, Yang C, Brinkman KL, Serrano-Gonzalez M, Jope RS, Zhou B, Engler DA, Zhan M, Wong ST, Fu L, Xu B. J Mol Cell Biol. 2012

5. Rettig GR, Behlke MA. Mol Ther. 2012; 20:483–512. [PubMed: 22186795]
6. a Ferrari M. Trends Biotechnol. 2010; 28:181–188. [PubMed: 20079548] b Shen H, Sun T, Ferrari M. Cancer Gene Ther. 2012
7. Tasciotti E, Liu X, Bhavane R, Plant K, Leonard AD, Price BK, Cheng MM, Decuzzi P, Tour JM, Robertson F, Ferrari M. Nat Nanotechnol. 2008; 3:151–157. [PubMed: 18654487]
8. van de Ven AL, Kim P, Haley O, Fakhoury JR, Adriani G, Schmulen J, Moloney P, Hussain F, Ferrari M, Liu X, Yun SH, Decuzzi P. J Control Release. 2011
9. a Epenetos AA, Snook D, Durbin H, Johnson PM, Taylor-Papadimitriou J. Cancer Res. 1986; 46:3183–3191. [PubMed: 3516393] b Khawli LA, Miller GK, Epstein AL. Cancer. 1994; 73:824–831. [PubMed: 8306266]
10. a Tanaka T, Mangala LS, Vivas-Mejia PE, Nieves-Alicea R, Mann AP, Mora E, Han HD, Shahzad MM, Liu X, Bhavane R, Gu J, Fakhoury JR, Chiappini C, Lu C, Matsuo K, Godin B, Stone RL, Nick AM, Lopez-Berestein G, Sood AK, Ferrari M. Cancer Res. 2010; 70:3687–3696. [PubMed: 20430760] b Ferrari M. Nat Rev Clin Oncol. 2010; 7:485–486. [PubMed: 20798696]
11. a Hornung V, Guenthner-Biller M, Bourquin C, Ablasser A, Schlee M, Uematsu S, Noronha A, Manoharan M, Akira S, de Fougerolles A, Endres S, Hartmann G. Nat Med. 2005; 11:263–270. [PubMed: 15723075] b Judge AD, Sood V, Shaw JR, Fang D, McClintock K, MacLachlan I. Nat Biotechnol. 2005; 23:457–462. [PubMed: 15778705]
12. Zhao F, Zhao Y, Liu Y, Chang X, Chen C. Small. 2011; 7:1322–1337. [PubMed: 21520409]
13. Shen H, You J, Zhang G, Ziemys A, Li Q, Bai L, Deng X, Erm DR, Liu X, Li C, Ferrari M. Adv Healthcare Mater. 2012; 1:84–89.
14. Tanaka T, Godin B, Bhavane R, Nieves-Alicea R, Gu J, Liu X, Chiappini C, Fakhoury JR, Amra S, Ewing A, Li Q, Fidler IJ, Ferrari M. Int J Pharm. 2010; 402:190–197. [PubMed: 20883755]
15. a Schulz O, Diebold SS, Chen M, Naslund TI, Nolte MA, Alexopoulou L, Azuma YT, Flavell RA, Liljestrom P, Reis e Sousa C. Nature. 2005; 433:887–892. [PubMed: 15711573] b Alexopoulou L, Holt AC, Medzhitov R, Flavell RA. Nature. 2001; 413:732–738. [PubMed: 11607032] c Tateda K, Matsumoto T, Miyazaki S, Yamaguchi K. Infect Immun. 1996; 64:769–774. [PubMed: 8641780]
16. a Ozato K, Tsujimura H, Tamura T. Biotechniques. 2002; (Suppl):66–68. 70, 72. passim. [PubMed: 12395929] b Oppenheim JJ. Adv Exp Med Biol. 1993; 351:183–186. [PubMed: 7942295]
17. a Degre M. Proc Soc Exp Biol Med. 1973; 142:1087–1091. [PubMed: 4694806] b Shiow LR, Rosen DB, Brdickova N, Xu Y, An J, Lanier LL, Cyster JG, Matloubian M. Nature. 2006; 440:540–544. [PubMed: 16525420]
18. a Alao JP, Sunnerhagen P. Radiat Oncol. 2009; 4:51. [PubMed: 19903334] b Rainey MD, Charlton ME, Stanton RV, Kastan MB. Cancer Res. 2008; 68:7466–7474. [PubMed: 18794134] c Hickson I, Zhao Y, Richardson CJ, Green SJ, Martin NM, Orr AI, Reaper PM, Jackson SP, Curtin NJ, Smith GC. Cancer Res. 2004; 64:9152–9159. [PubMed: 15604286]
19. Pellegrini M, Celeste A, Difilippantonio S, Guo R, Wang W, Feigenbaum L, Nussenzweig A. Nature. 2006; 443:222–225. [PubMed: 16906133]
20. Ivanov VN, Zhou H, Partridge MA, Hei TK. Cancer Res. 2009; 69:3510–3519. [PubMed: 19351839]
21. Li Y, Yang DQ. Mol Cancer Ther. 2010; 9:113–125. [PubMed: 20053781]
22. Spring K, Ahangari F, Scott SP, Waring P, Purdie DM, Chen PC, Hourigan K, Ramsay J, McKinnon PJ, Swift M, Lavin MF. Nat Genet. 2002; 32:185–190. [PubMed: 12195425]
23. Pharoah PD, Day NE, Caldas C. Br J Cancer. 1999; 80:1968–1973. [PubMed: 10471047]
24. Soussi T. Ann N Y Acad Sci. 2000; 910:121–137. discussion 137-129. [PubMed: 10911910]
25. Mitchell LA, Lauer FT, Burchiel SW, McDonald JD. Nat Nanotechnol. 2009; 4:451–456. [PubMed: 19581899]

26. a Walter S, Bottazzi B, Govoni D, Colotta F, Mantovani A. Int J Cancer. 1991; 49:431–435. [PubMed: 1655661] b Baay M, Brouwer A, Pauwels P, Peeters M, Lardon F. Clin Dev Immunol. 2011; 2011:565187. [PubMed: 22162712]

27. Serda RE, Mack A, van de Ven AL, Ferrati S, Dunner K Jr. Godin B, Chiappini C, Landry M, Brousseau L, Liu X, Bean AJ, Ferrari M. Small. 2010; 6:2691–2700. [PubMed: 20957619]

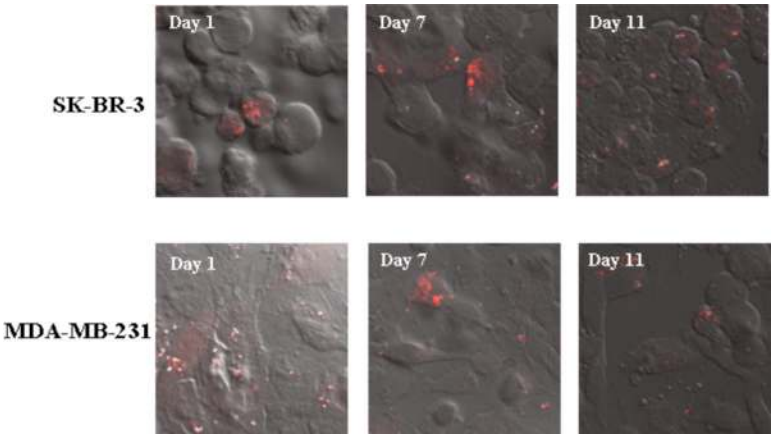

Figure 1. Sustained release of siRNA from MSV in human breast cancer cells

MDA-MB-231 and SK-BR-3 breast cancer cells were incubated with MSV/Alexa555-siRNA. Images of both the MSV particles and fluorescent siRNA were captured 1, 7 and 11 days by confocal microscope. Representative confocal images are displayed.

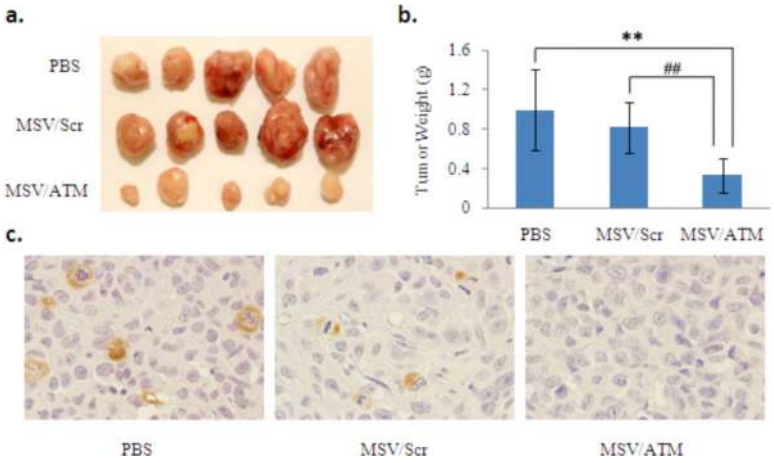

Figure 2. MSV/ATM treatment knocks down ATM expression and inhibits tumor growth in MDA-MB-231 xenograft model

MDA-MB-231 cells (3×10^6) were inoculated into the mammary fat pad of nude mice ($n = 5$). Mice were treated biweekly with PBS, MSV/Scr (15 μg siRNA) or MSV/ATM (15 μg siRNA) when average tumor size reached 150 – 200 mm^3. (*a*) Images of MDA-MB-231 tumor tissues at the end of the treatment. (b) Tumor weight measurement. ** $P < 0.01$vs PBS, ## $P < 0.01$vs MSV/Scr. (c) Immunohistochemical analysis of ATM expression in MDA-MB-231 tumor samples (600× magnification).

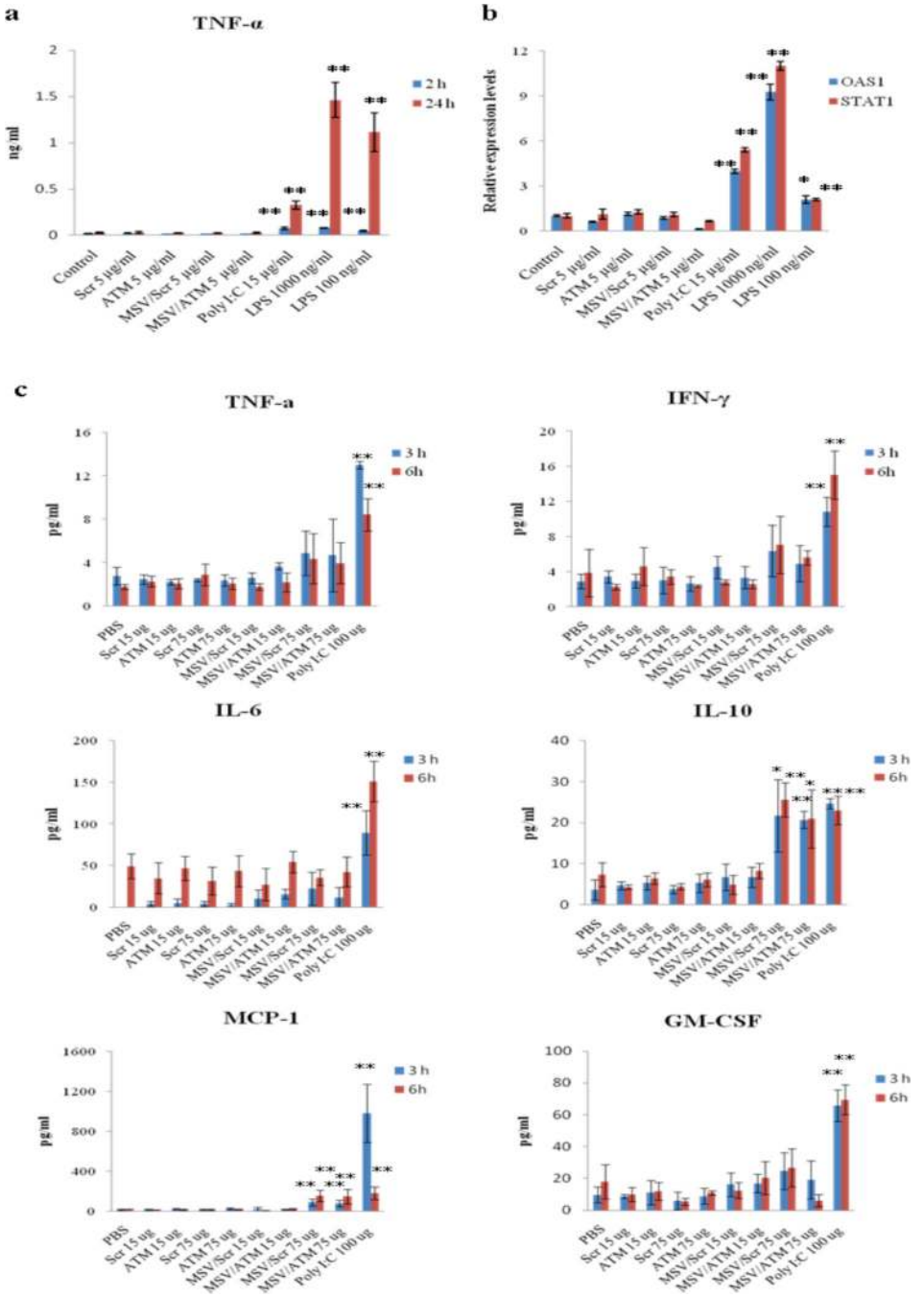

Figure 3. MSV/ATM does not induce innate immune response *in vitro* or *in vivo*

Raw-264.7 mouse macrophage cells were incubated with indicated agents for 2 or 24 hours, and a) TNF- level in supernatant was measured by ELISA. **P <0.01. b) OAS1 and STAT1 mRNA levels were measured by quantitative real-time PCR, and normalized to actin. The expression levels are presented as a fraction of values from the untreated cells. *P <0.05, **P <0.01. c) Changes in levels of selected serum cytokine/chemokine/colony-stimulating factors in post-treatment mice. Blood samples were collected 3 or 6 hours after dosing of treatment agents. A multiplexed bead-based immunoassay was used to measure levels of 32 cytokines/chemokines/colony-stimulating factors. *P <0.05. **P <0.01.

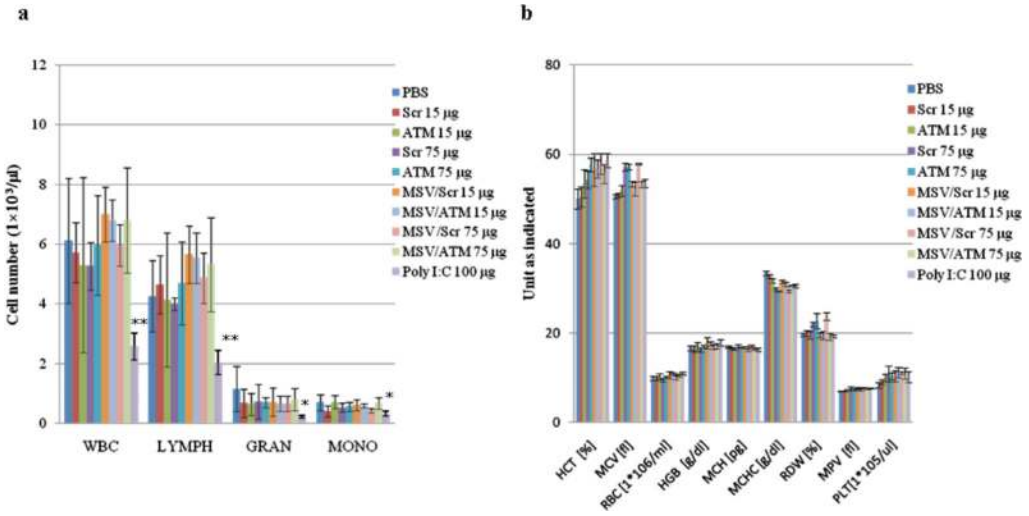

Figure 4. Hematological analysis for evaluation of sub-acute toxicity

Mice were treated once per week for 4 weeks with the indicated agents, and blood samples were collected 24 hours after the last dosing for hematological analysis. Results are displayed as average ± SD (n=5). a) Changes in white blood cell (WBC), lymphocyte (LYMPH), granulocyte (GRAN), and monocyte (MONO). b) Changes in red blood cell (RBC), hematocrit (HCT), hemoglobin (HGB) concentration, and MCV, MCH, MCHC, MPV, RDW, and platelet count. *P <0.05. **P <0.01.

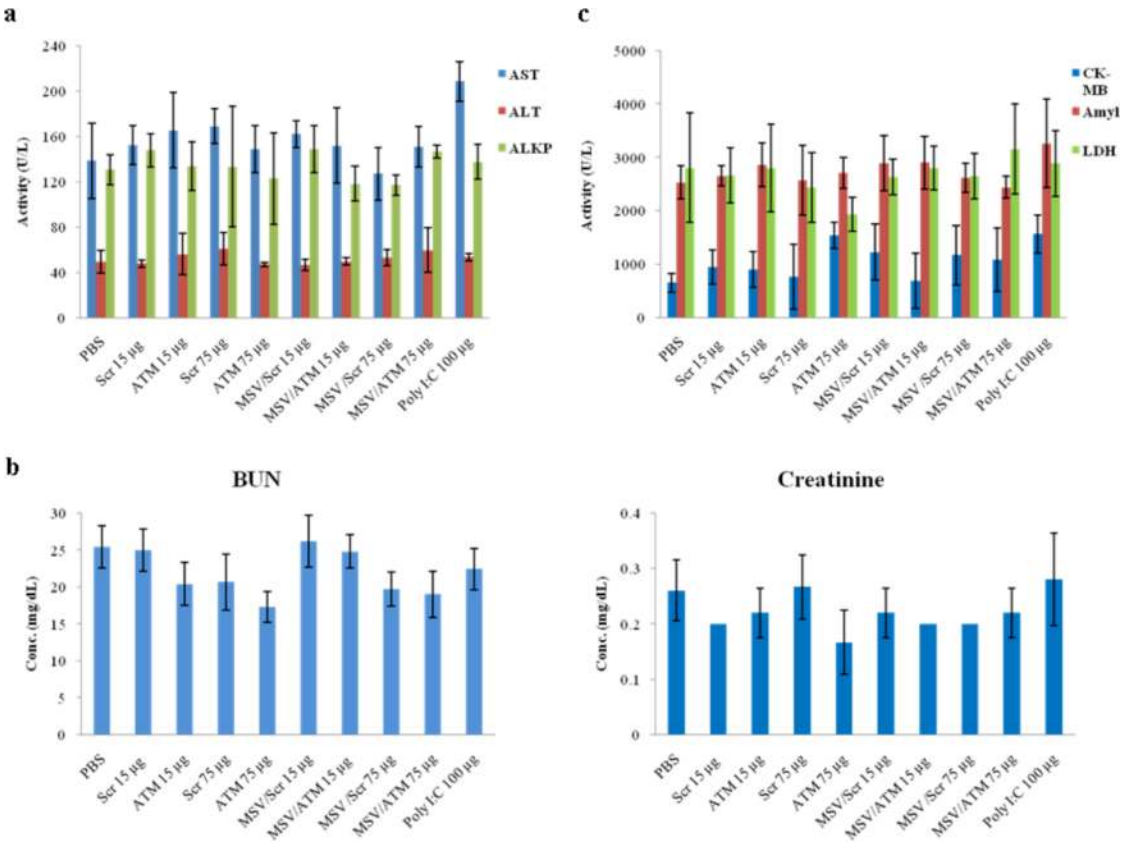

Figure 5. Blood biochemistry analysis for evaluation of sub-acute toxicity

Serum samples were collected from mice after 4 weeks of treatment, and levels of a) hepatic enzymes [alkaline phosphatase (ALKP), alanine aminotransferase (ALT), and aspartate aminotransferase (AST)], b) renal function biomarkers [blood urea nitrogen (BUN), creatinine], and c) other biomarkers [amylase (Amyl), creatinine kinase MB (CKMB), lactate dehydrogenase (LDH)] were measured. Each value represents the mean ± SD (n=5).

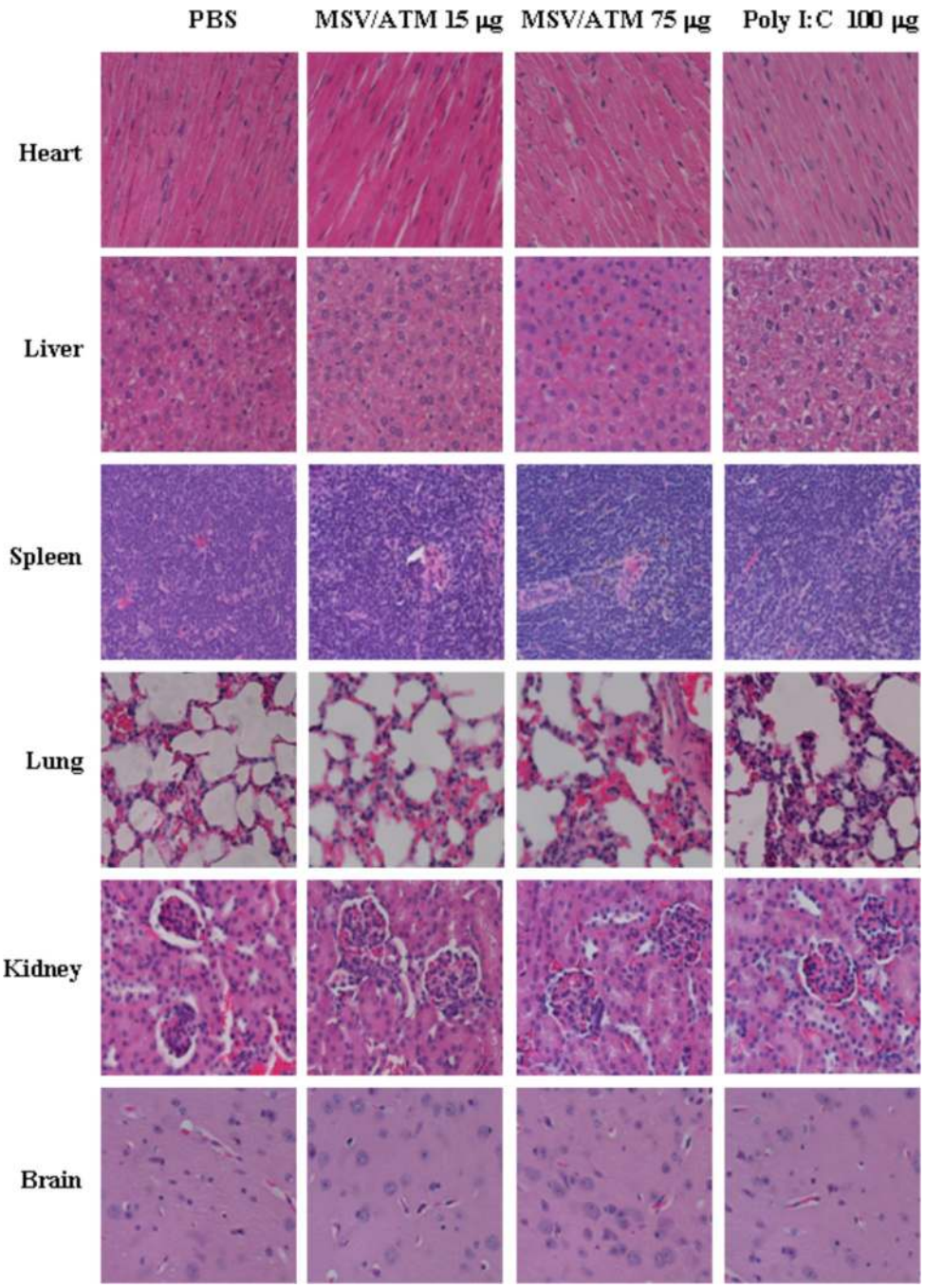

Figure 6. Histopathological examination of major organs for evaluation of sub-acute toxicity

Major organs were collected after 4 weeks of treatment, and analyzed for potential tissue damages by H&E staining. Representative images (400×) of heart, liver, spleen, lung, kidney and brain from mice in the control groups (PBS, Poly I:C 100 □g) and treatment groups (MSV/ATM 15 □g, MSV/ATM 75 □g) are shown. Each picture is a representative of at least five independent sections.

Table 1

Characterization of liposomal ATM siRNA and MSV/ATM.

	Liposome/ATM	MSV	MSV/ATM
Size	112 nm	1 □m	1 □m
Z-potential (mV)	−1.78 mV	+4.0 mV	−21.14 mV

Table 2

Coefficients of liver, kidney and spleen after four weeks of treatment

Groups	Body Weight (g)		Liver (mg/g)	Spleen (mg/g)	Kidney (mg/g)
	Before treatment	After treatment			
PBS	18.8 ± 0.89	19.9 ± 0.52	50.9 ± 5.89	5.16 ± 0.58	12.4 ± 0.92
Scr 15 μg	18.8 ± 0.26	19.7 ± 0.6	51.9 ± 7.41	5.13 ± 0.18	11.6 ± 0.38
ATM 15 μg	18.3 ± 0.32	19.2 ± 0.53	53.5 ± 4.65	5.03 ± 0.26	12.2 ± 0.88
Scr 75 μg	17.9 ± 0.79	19.7 ± 0.51	50.4 ± 3.84	5.07 ± 0.32	11.7 ± 0.63
ATM 75 μg	18.0 ± 0.51	19.7 ± 0.66	51.6 ± 4.83	4.96 ± 0.46	11.6 ± 0.52
MSV/Scr 15 μg	18.8 ± 0.94	19.7 ± 0.51	48.2 ± 6.64	5.30 ± 0.60	11.6 ± 0.43
MSV/ATM 15 μg	19.2 ± 0.93	20.2 ± 0.96	52.8 ± 2.61	5.00 ± 0.12	11.2 ± 0.30
MSV/Scr 75 μg	17.8 ± 0.48	19.8 ± 0.71	50.5 ± 3.16	5.02 ± 0.38	11.7 ± 0.66
MSV/ATM 75 μg	18.8 ± 0.68	20.0 ± 0.71	50.8 ± 3.09	5.00 ± 0.38	11.3 ± 0.55
Poly I:C 100 μg	18.4 ± 0.43	19.7 ± 0.80	50.7 ± 4.17	5.92 ± 0.50	12.0 ± 0.79